Environmental Microbiology (1999) **1**(5), 447–455

The formation of migratory ripples in a mixed species bacterial biofilm growing in turbulent flow

Paul Stoodley,[1]* Zbigniew Lewandowski,[2] John D. Boyle[3] and Hilary M. Lappin-Scott[1]
[1]Exeter University, School of Biology, Hatherly Laboratories, Prince of Wales Road, Exeter EX4 4PS, UK.
[2]Center for Biofilm Engineering, 366 EPS Building – PO Box 173980, Montana State University-Bozeman, Bozeman, MT 59717-3980, USA.
[3]Exeter University, School of Engineering and Computer Science, North Park Road, Exeter EX4 4QF, UK.

Summary

Mixed-species biofilms, consisting of *Klebsiella pneumoniae*, *Pseudomonas aeruginosa*, *Pseudomonas fluorescens* and *Stenotrophomonas maltophilia*, were grown in glass flow cells under either laminar or turbulent flow. The biofilms grown in laminar flow consisted of roughly circular-shaped microcolonies separated by water channels. In contrast, biofilm microcolonies grown in turbulent flow were elongated in the downstream direction, forming filamentous 'streamers'. Moreover, biofilms growing in turbulent flow developed extensive patches of ripple-like structures between 9 and 13 days of growth. Using time-lapse microscopic imaging, we discovered that the biofilm ripples migrated downstream. The morphology and the migration velocity of the ripples varied with short-term changes in the bulk liquid flow velocity. The ripples had a maximum migration velocity of 800 $\mu m\,h^{-1}$ ($2.2 \times 10^{-7}\,m\,s^{-1}$) when the liquid flow velocity was $0.5\,m\,s^{-1}$ (Reynolds number = 1800). This work challenges the commonly held assumption that biofilm structures remain at the same location on a surface until they eventually detach.

Introduction

Characklis (1981) identified three key processes in the life cycle of biofilms. Planktonic microbial cells attach to a solid surface (substratum). The biomass accumulates on the surface as the attached cells divide and produce an extracellular polysaccharide (EPS) slime matrix. Finally, both single cells (erosion) and large pieces of biofilm (sloughing) detach from the surface. These assumptions are reflected in biofilm mass balance equations (Characklis, 1990) and mathematical models (Reichert and Wanner, 1997; Picioreanu *et al*., 1998). These models implicitly assume that, as biofilm microcolonies grow, they remain at the same location on the substratum until they eventually detach (Palmer and White, 1997). The idea that biofilm structures remain at a specific location on the substratum has persisted for a number of reasons. First, biofilms are usually inspected *ex situ* on surfaces that have been removed from flowing systems. Secondly, where flow cells have been used, studies are generally limited to low laminar flows. Thirdly, very few, if any, studies have used long-term, time-lapse microscopic imaging to observe biofilm behaviour in turbulent flows. A few studies have reported various structural features in biofilms, such as ripples and dunes, which suggest the possibility of surface transport mechanisms, but no details on the behaviour of these structures have been given (Gjaltema *et al*., 1994; Stoodley *et al*., 1997). A better understanding of biofilm behaviour is particularly important because of the many problems associated with biofilm colonization, ranging from medical infections (Hoiby *et al*., 1995; Foley and Gilbert, 1996) to the fouling of industrial components (Lappin-Scott and Costerton, 1989; Costerton *et al*., 1995).

It was the goal of our work to document the formation and differences in structures in a mixed species biofilm growing in either laminar or turbulent flow and to determine the influence of short-term changes in the hydrodynamic conditions on biofilm morphology and behaviour.

Results

Biofilm growth conditions

We grew mixed-species biofilms using an inoculum containing *Pseudomonas aeruginosa* (ERC1), *Pseudomonas fluorescens*, *Klebsiella pneumoniae* and *Stenotrophomonas maltophilia*. Biofilms were grown in either laminar or turbulent flow in square glass tubing flow cells (Fig. 1) for between 18 and 23 days in triplicate experiments. The flow velocity (u) in the laminar flow cell was maintained at $0.03\,m\,s^{-1}$ with a corresponding Reynolds number (Re, based on channel hydraulic diameter) of 120. In

Received 12 March, 1999; revised 8 June, 1999; accepted 11 June, 1999. *For correspondence. E-mail p.stoodley@exeter.ac.uk; Tel. (+44) 1392 264348; Fax (+44) 1392 263700.

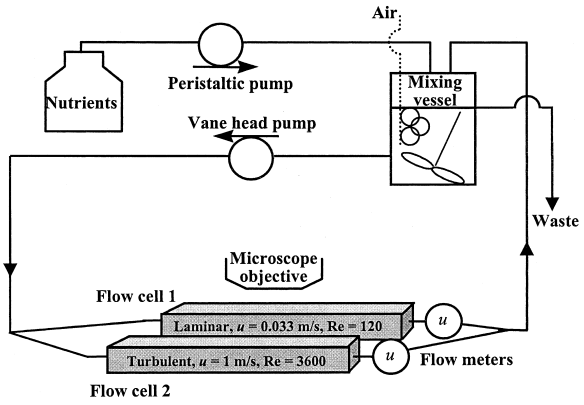

Fig. 1. Biofilm reactor system after Stoodley *et al.* (1999c), consisting of two glass flow cells in parallel that were incorporated into a recirculating loop attached to a mixing vessel to which nutrients and air were added. The level was maintained by overflow to waste. The flow cells were held in a polycarbonate holder and positioned on the microscope stage for *in situ* imaging.

the turbulent flow cell, u was 1 m s^{-1} and *Re* 3600. Pressure drop data showed that the transition point between laminar and turbulent flow occurred at approximately *Re* 1200 (Stoodley *et al.*, 1999a). Under these conditions, the theoretical wall shear stresses in the laminar and turbulent flow cells were 0.074 and 5.09 N m^{-2} respectively.

Concentration and proportions of bacterial species in the biofilms

The average surface concentration of biofilm cells in the laminar and turbulent flow cells was $8.5 \pm 0.3 \times 10^7$ ($n = 6$) and $1.4 \pm 0.5 \times 10^8$ ($n = 9$) cfu cm^{-2} respectively. These values were not significantly different at the 95% level ($P = 0.16$, ANOVA, $n = 15$).

The proportions of species in the bulk liquid and both the laminar and the turbulent biofilms were also similar and dominated by *K. pneumoniae* (*c.* 90%) (Table 1).

Biofilm structure in laminar and turbulent flow

After 9 days, the biofilm in the laminar flow cell was heterogeneous and consisted of microcolonies separated by interstitial channels. The microcolonies were roughly circular in shape and up to 100 μm in diameter. In the channel areas, there was a sparse covering of single cells on the glass surface. The biofilm grown in turbulent flow also had a heterogeneous structure of microcolonies. However, the larger microcolonies (diameter >40 μm) were elongated in the downstream direction, forming filamentous streamers (Stoodley *et al.*, 1998; 1999b). The upstream 'heads' of the streamers were attached to the substratum, while the 'tails' were free to oscillate in the flow. Single cells were attached to the substratum in the channels surrounding the streamers. Some of the cells appeared to be firmly attached, but others were transported downstream at a velocity of 14 ± 1 μm h^{-1} ($3.9 \pm 0.3 \times 10^{-9}$ m s^{-1}) (mean ± 1 SE, $n = 5$). Between days 9 and 13, extensive patches of ripple-like structures (hereafter referred to as ripple beds) had formed on both the upper and the lower surfaces of the turbulent flow cells in all three runs (Fig. 2A). The larger ripple beds were of the order of 1 mm wide and over 3 mm in length. Individual ripples within the ripple beds were up to 250 μm long and 50 μm wide. The ripples were made up of dense aggregates of bacterial cells (Fig. 2B). In between the ripples were trough areas in which there was a layer of single cells on the substratum. Ripple structures did not form in the laminar flow cells over the course of the experiments (Fig. 2C).

Morphology and migration of biofilm ripples

Time-lapse imaging in the turbulent flow cell for periods of up to 24 h showed that the ripples migrated downstream at an average velocity of 23 ± 6 μm h^{-1} ($6.4 \pm 1.7 \times 10^{-9}$ m s^{-1}) ($n = 5$ individual ripples in different ripple patches). The ripples moved over single cells on the glass surface and small (diameter <40 μm) cell clusters that were firmly attached to the surface. The downstream migration of one ripple bed was tracked by measuring the position of the advancing front of the ripple bed over a 24 h period, during which the ripple bed migrated downstream at a constant velocity of 17 μm h^{-1} (4.7×10^{-9} m s^{-1}) ($r^2 = 0.997$, $n = 13$) (Fig. 3). While some of the ripple beds advanced steadily downstream, other ripple beds had a well-defined

Table 1. Viable suspended and biofilm cell concentrations averaged from the three experimental runs.

Species	Suspended (cfu ml^{-1})	Laminar biofilm (cfu cm^{-2})	Turbulent biofilm (cfu cm^{-2})
Pseudomona aeruginosa	$7.2 \pm 2.2 \times 10^6$ (15.1%)	$5.2 \pm 1.0 \times 10^6$ (6.0%)	$1.6 \pm 0.6 \times 10^7$ (7.9%)
Pseudomonas fluorescens	$7.0 \pm 0.6 \times 10^5$ (2.1%)	$1.1 \pm 0.3 \times 10^6$ (0.6%)	$4.3 \pm 1.6 \times 10^6$ (2.2%)
Klebsella pneumoniae	$3.3 \pm 0.6 \times 10^7$ (79.6%)	$7.6 \pm 0.2 \times 10^7$ (91.0%)	$1.1 \pm 0.4 \times 10^8$ (88.0%)
Stenotrophomonas maltophilia	$1.2 \pm 0.2 \times 10^6$ (3.3%)	$2.0 \pm 0.5 \times 10^6$ (2.4%)	$3.1 \pm 1.4 \times 10^6$ (1.9%)
Total	$4.2 \pm 0.8 \times 10^7$	$8.4 \pm 0.3 \times 10^7$	$1.4 \pm 0.5 \times 10^8$

Data were collected at the end of each run. For the suspended and turbulent biofilm data, $n = 9$ and, for the laminar biofilm data, $n = 6$ based on triplicate plate counts per run. The relative proportion of the individual species to the total population is shown as a percentage.

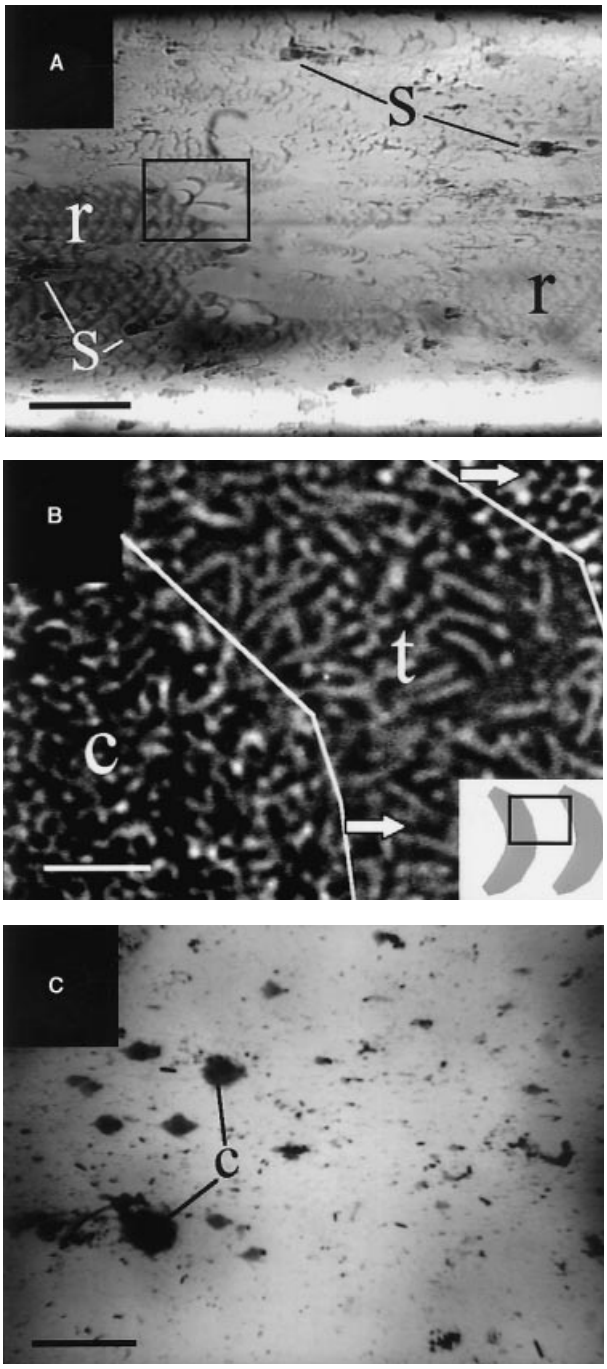

downstream terminus at which individual ripples regularly detached into the bulk liquid (Fig. 4). This had the effect that, although individual ripples were constantly migrating downstream, there was no net downstream movement of the ripple bed.

The morphology of the ripples and their migration velocity varied with short-term changes in the *Re* of the bulk liquid (Figs 5 and 6). At a *Re* of 4200 ($u = 1.17\,m\,s^{-1}$), the ripples in a monitored ripple bed were aligned in parallel, perpendicular to the bulk liquid flow direction (Fig. 5A). The wavelength (peak to peak distance) was $\approx 75\,\mu m$ (Fig. 6A). However, when the *Re* of the bulk liquid was reduced to 1200 ($u = 0.33\,m\,s^{-1}$), the ripples became markedly more curved (Fig. 5B), and the ripple wavelength increased to $\approx 200\,\mu m$ (Fig. 6B). When the *Re* was changed, it took less than 1 h for the ripples in the monitored ripple bed to restabilize to the new configuration. The height of the ripples decreased from $\approx 50\,\mu m$ at R*e* 1200 ($u = 0.33\,m\,s^{-1}$) to a minimum of $10\,\mu m$ at *Re* 3000 ($u = 0.83\,m\,s^{-1}$) (Fig. 6B). A maximum migration velocity of $800\,\mu m\,h^{-1}$ ($2.2 \times 10^{-7}\,m\,s^{-1}$) occurred at *Re* 1800 ($u = 0.5\,m\,s^{-1}$). Figure 7 illustrates the downstream motion of individual ripples over the glass surface at *Re* 2400. Some of the smaller microcolonies (diameter $< 20\,\mu m$) were also transported downstream along the glass surface ($15 \pm 3\,\mu m\,h^{-1}$, $n = 5$ different microcolonies) (Fig. 7). Time-lapse monitoring over periods of up to 14 h in the laminar flow experiments revealed no downstream transport of biofilm microcolonies.

Viable cell concentration in the ripple patches

The surface viable cell concentration in the ripple patches was $\approx 1.4 \pm 0.3 \times 10^9$ cfu cm^{-2} ($n = 2$). The species proportions (*P. aeruginosa* 4.8%; *P. fluorescens* 7.4%; *K. pneumoniae* 86.5%; and *S. maltophilia* 1.3%) were similar to those in the total biofilm population (see Table 1).

Discussion

Influence of hydrodynamics on biofilm structure

Biofilms were grown in parallel flow cells under either laminar or turbulent flow and observed *in situ*. The structure

Fig. 2. A. Low-magnification photomicrograph of a biofilm growing in a turbulent flow cell (image from run 2 after 15 days of growth) showing ripple beds (r) and streamers (s). Time-lapse imaging showed that individual ripples within the ripple beds constantly moved downstream. In the labelled ripple bed on the left of the image, individual ripples detached when they reached the front of the ripple bed. Ripples detaching from the region within the box are shown in Fig. 4. Because of the continual detachment of ripples, this particular ripple bed had not advanced downstream over a 7.5 h monitoring period. Scale bar = 500 μm. A video of the ripple movement can be found on the journal's website (http://www.blackwell-science.com/emi). Liquid flow was from left to right in all photomicrographs.
B. High magnification of two of the ripples shown in (A) showed that the ripples were made up of dense aggregates of cells. At the high point (or crest 'c'), the ripples were ≈ 20 μm thick. Live imaging showed that the cells within the ripple were constantly twitching, so that the cells in these areas appear blurred. Single cells were attached to the glass surface in the troughs 't' between the ripples. The edges of the two ripples in the frame have been outlined for clarity, and the inset shows the relative location of the frame with respect to the two ripples. The arrows indicate the direction of the bulk liquid flow and ripple migration. Scale bar = 10 μm.
C. The biofilms grown in laminar flow (image from run 1 after 18 days' growth) consisted of microcolonies 'c' separated by interstitial voids. Scale bar = 500 μm.

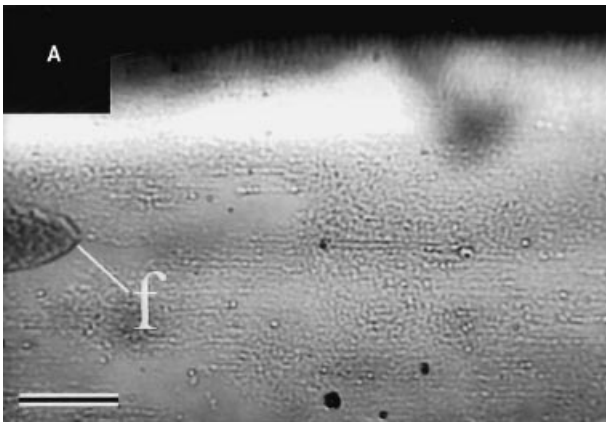

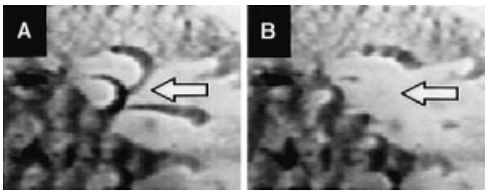

Fig. 4. Enlarged view of the boxed region in Fig. 2A showing ripple detachment.
A. The arrow indicates two large ripples at the front of the ripple bed. The club-shaped structure directly below the arrow is a ripple from which the lower arm had detached before the image was captured.
B. The following frame after 15 min showed that the ripples had detached from the surface. Box length = 500 μm.

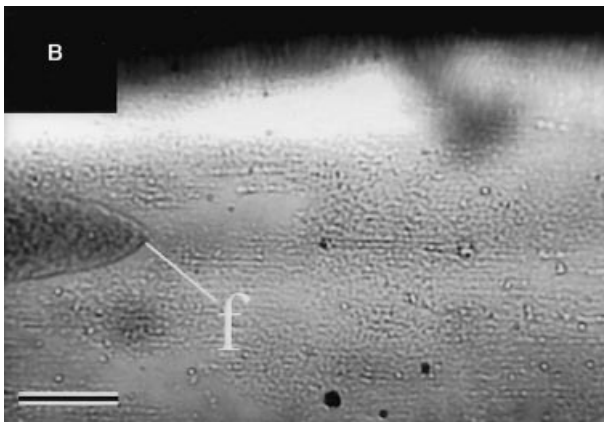

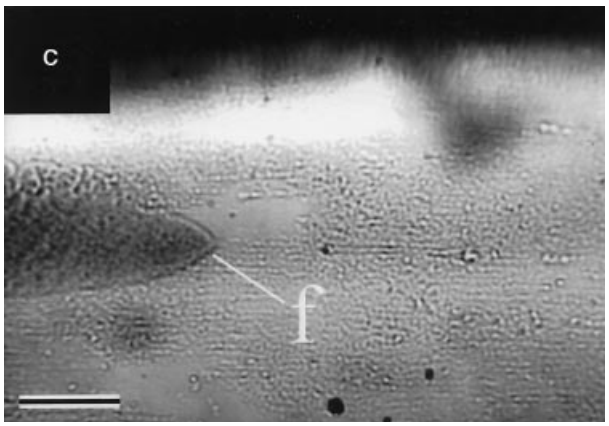

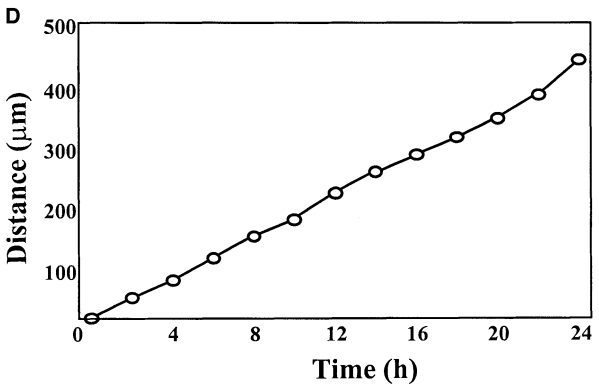

and behaviour of the biofilms was different depending on the two flow conditions. As both biofilm populations had a similar composition and nutrient conditions were identical, it is reasonable to conclude that the structural differences were a result of the different hydrodynamic conditions in the laminar and turbulent flow cells. In the laminar flow cells, the biofilm consisted of approximately circular microcolonies separated by interstitial channels. Similar structures have been described in detail using confocal scanning laser microscopy (Caldwell *et al*., 1993; deBeer *et al*., 1994; Massol-Deya *et al*., 1994; Møller *et al*., 1998), and it is the data from these and other studies that form the basis for recent conceptual depictions of biofilm structure (Costerton *et al*., 1995; Palmer and White, 1997). However, these and most other studies on biofilms growing *in situ* have been conducted on biofilms growing in laminar flows, and the influence of turbulent flow has been largely neglected. In turbulent flow, the biofilm microcolonies can become elongated to form filamentous streamers. In previous work, we speculated that such streamers might be formed by the influence of hydrodynamic drag on the developing biofilm microcolonies (Stoodley *et al*., 1998; 1999b). Similar filamentous structures have also been reported by others for biofilms grown in turbulent flow (Bryers and Characklis, 1981; McCoy *et al*., 1981; Picologlou *et al*., 1980).

In addition to the streamers, the biofilms grown in turbulent flow also formed patches of ripple-like structures that

Fig. 3. Downstream migration of a biofilm ripple bed in turbulent flow (from R3 on day 13) illustrated by a time sequence of images after 0 (A), 6 (B) and 12 h (C). The flow velocity of the bulk liquid was 1 m s^{-1}. The advancing front of the ripple bed 'f' is indicated by an arrow. The microscope settings were adjusted to maximize the contrast of the edge of the ripple bed. Individual ripples within the ripple bed were difficult to distinguish under these settings. Scale bars = 200 μm.
D. Distance travelled by the advancing front of the ripple bed measured over time showed that the ripple bed migrated downstream at a constant velocity of 17 μm h^{-1} (4.7×10^{-9} m s^{-1}) over a 24 h period.

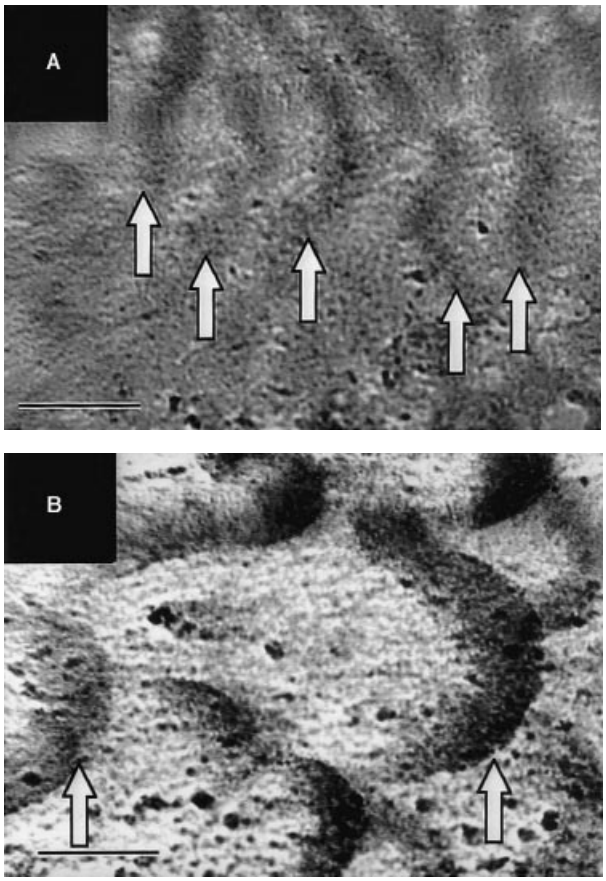

Fig. 5. The ripple morphology varied with short-term changes in the bulk liquid *Re*.
A. At *Re* 4200 ($u = 1.17\,m\,s^{-1}$), the ripples were relatively straight and aligned perpendicularly to the bulk liquid flow direction. Individual ripples are indicated by the arrows.
B. When the *Re* was reduced to 1800 ($u = 0.5\,m\,s^{-1}$), the ripples became more curved, and the spacing (wavelength) between them increased. Scale bars = 100 μm.

were distributed throughout the flow cell. These structures were similar to those reported by Gjaltema *et al*. (1994), who grew pure culture *P. aeruginosa* biofilms in turbulent flow in an annular reactor. However, as their biofilms were removed from the bulk liquid for microscopic examination, they were unable to see any direct evidence of movement of these structures.

Influence of hydrodynamics on biofilm behaviour

Time-lapse imaging showed that both biofilm ripples and clusters moved downstream along the surface of the turbulent flow cell. Some of the ripples regularly detached from the front of some of the ripple beds into the bulk liquid. It was not clear why there was detachment from some ripple beds but not others or what caused the detachment. It is possible that the detachment may be related to either the variation in surface chemistry of the glass (i.e. location dependent) or the ageing of the biofilm ripples as they migrate (i.e. time dependent). Such continual detachment of biofilm is of particular concern to the food (Carpentier and Cerf, 1993) and water industries, in which product contamination by sloughed microcolonies may result in spoilage and, more importantly, the potential transmission of pathogens (Buswell *et al*., 1998).

In addition to the long-term influence of hydrodynamics on the development of biofilm structure, we looked at the effect of short-term changes resulting from varying the velocity of the bulk liquid. Both the ripple morphology and the migration velocity responded within minutes to changes in flow velocity. This rapid response suggests

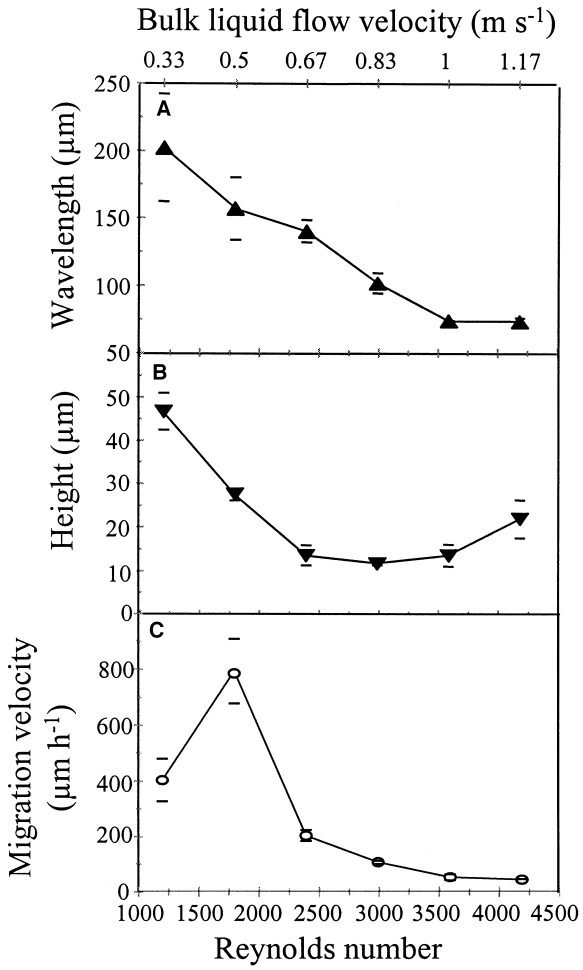

Fig. 6. Influence of short-term changes in bulk liquid *Re* on biofilm morphology and migration velocity (bars = 1 SE, *n* = number of different ripples measured).
A. The ripple wavelength decreased as *Re* increased ($n = 3$).
B. The height of the ripples declined as *Re* increased and reached a minimum of 12 μm at about *Re* 2400 ($n = 3$).
C. The ripple migration velocity had a maximum of 800 $\mu m\,h^{-1}$ ($2.2 \times 10^{-7}\,m\,s^{-1}$) when the *Re* in the flow cell was 1800 ($u = 0.5\,m\,s^{-1}$) ($n = 5$). The data were collected from the same area of the ripple bed shown in Fig. 5 over a period of 18 h.

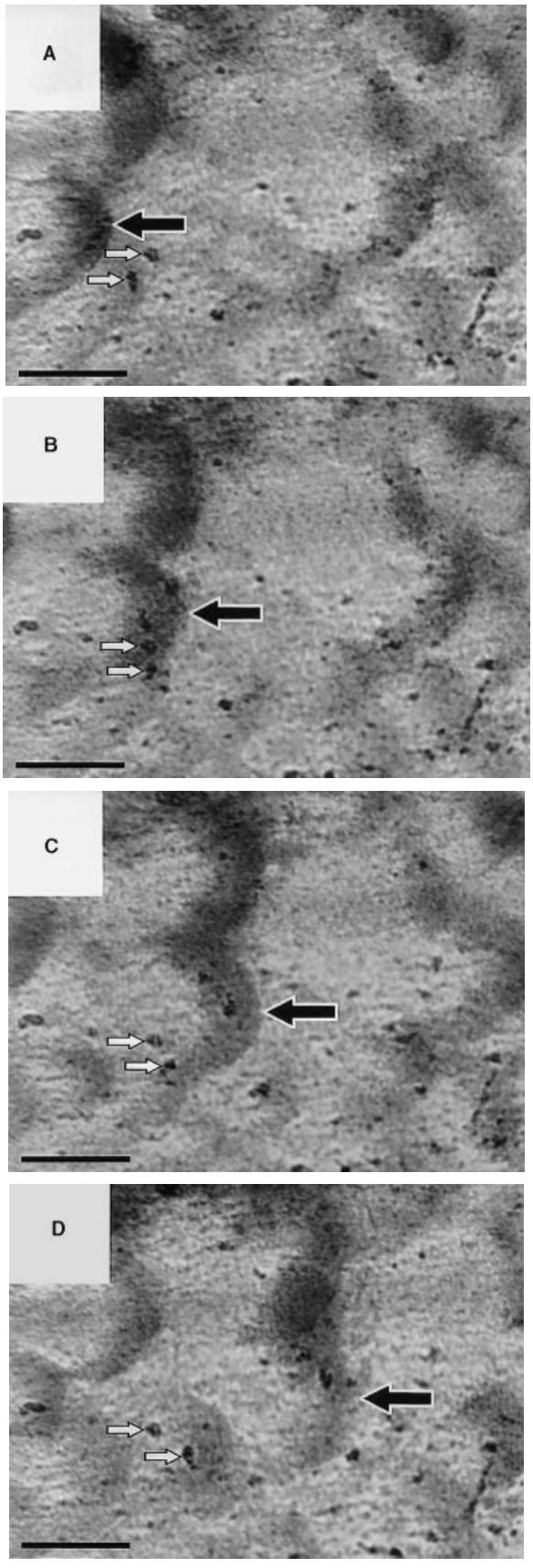

that the observed morphological changes may result largely from the physical hydrodynamic forces acting on the biofilm. In a parallel study, we have investigated the rheology of the four species biofilm by monitoring the contractions and extensions in microcolony length caused by changes in bulk fluid shear stress (Stoodley *et al.*, 1999a,c). We found that the biofilm was a compliant viscoelastic material that was readily deformed by changes in fluid shear. Also, when fluid shear was increased above a threshold value, the biofilm behaved like a viscoelastic liquid and began to flow. It is possible that the formation of migrating ripples could be caused by the biofilm flowing under certain hydrodynamic conditions. The compliance of the material may also explain the morphological changes in response to varying bulk liquid flow velocity. As the drag coefficient is shape and size dependent (Vogel, 1994), this may help to explain the unexpected observation that the ripple migration velocity decreased when the bulk liquid *Re* was increased above *Re* 1800. Further work is required to elucidate the exact nature and mechanisms of ripple motion.

The transport of biofilm structures across the surface in the turbulent flow cells contrasted with the laminar experiments in which time-lapse monitoring of periods up to 14 h revealed no such downstream transport of biofilm microcolonies. It is possible that the biofilm structures grown in laminar flow may migrate, but at much slower velocities. Nutrient conditions may also play an important role in the transport of biofilm along solid surfaces. Thicker biofilms grown under higher nutrient conditions may have different coefficients of drag and behave differently from the structures that we observed.

Concluding remarks

Our work demonstrates the complexity of both long- and short-term interactions between the observed bacterial biofilms and the hydrodynamic conditions of the growth environment. Differences in both the structure and the temporal behaviour of biofilms grown under laminar flow compared with turbulent flow clearly indicate the importance of hydrodynamics in shaping the developing biofilm.

Fig. 7. Time-lapse sequence showing the movement of ripples across the flow cell surface after 0 (A),10 (B), 20 (C) and 50 min (D) at a bulk liquid *Re* of 2400 ($u = 0.67\,m\,s^{-1}$). One of the advancing ripples is indicated by the black arrow. It is also interesting to note that this ripple passed over two small microcolonies shown by the smaller white arrows. The microcolony indicated by the upper arrow remained at the same place, while the one indicated by the lower arrow moved downstream, but at a slower velocity than the ripple. The ripple velocity was $\approx 250\,\mu m\,h^{-1}$ ($6.9 \times 10^{-8}\,m\,s^{-1}$). The area in the photomicrograph overlaps with that shown in Fig. 5. Scale bar = 100 μm.

In laminar flow, the microcolonies were roughly circular. These forms are consistent with biofilms growing in conditions in which there are no significant variations in nutrient concentration and fluid shear around the microcolonies. However, under turbulent flow, the influence of the unidirectional shear became apparent, and the biofilm formed elongated streamers and ripples. Furthermore, time-lapse imaging revealed the dynamic nature of the biofilms growing in turbulent flow. The formation of ripples and our discovery that biofilm structures can be transported along a surface may fundamentally change our understanding of how biofilms behave in turbulent flow. This has important consequences for surface colonization and mass transfer processes occurring in biofilm systems. The observation that ripples, containing potentially large numbers of viable microorganisms, can continually detach into the bulk liquid also has serious implications for microbiological contamination from solid surfaces.

Recently, it has been demonstrated that concentration-dependent cell-signalling molecules (quorum sensing) may play an important role in the structural arrangement of pure culture *P. aeruginosa* biofilms (Davies *et al*., 1998). It was postulated that the biofilm structure may be controlled by attached bacteria to maximize the nutrient supply to the biofilm cells. Our observations suggest that complex organization in biofilms may also occur as a result of the hydrodynamic interactions between the bulk liquid and the biofilm material. In addition to the physical influence of drag on the biofilm and the transport of nutrients to the biofilm cells, hydrodynamics may also influence quorum-sensing processes by affecting the concentration of signalling molecules.

Experimental procedures

Biofilm reactor system

The reactor system consisted of two square glass tubing flow cells (20 cm lengths of 3×3 mm tubing supplied by Camlab Ltd), which were incorporated into a recirculation loop connected to a mixing chamber (Fig. 1). The system is described in greater detail elsewhere (Stoodley *et al*., 1999b). Nutrients were delivered by peristaltic pump (Masterflex; Cole Parmer), and the recycle flow rate was controlled by a vane head pump (Masterflex; Cole Parmer). The volume of the mixing chamber and recycle loop, including the flow cells, was 175 ml. The nutrient influent flow rate was 4.3 ml m^{-1}, giving a resulting residence time in the entire system of 40 min. The flow velocity through each of the flow cells was controlled independently by tightening or loosening clamps on the inlet tubing and measured using flow meters (McMillan Flo-sensor model 101T nos. 3724 and 3835 supplied by Cole-Parmer). Three experimental runs (R1, R2 and R3) were performed in which biofilms were grown for 18, 26 and 23 days respectively. For R2, the laminar flow cell was broken at day 6, so that data were only available for the turbulent flow cell during this run. The influence of short-term changes in fluid velocity on the structure and behaviour of the biofilm ripples that formed in the turbulent flow cell was investigated during R2 on days 18 and 19. An individual ripple bed positioned on the upper surface of the flow cell was selected and observed while the flow velocity of the bulk liquid was varied stepwise between 0.33 m s^{-1} (*Re* 1200) and 1.17 m s^{-1} (*Re* 4200). The biofilm ripple bed was monitored for 3 h at each velocity increment. Under operating conditions, the water temperature in the reactor system was 28 ± 2°C, and all experiments were performed at this temperature.

Reactor sterilization

The reactor system and nutrients were sterilized by autoclaving at 121°C for 15 min. The flow meters were sterilized using a method adapted from Fisher and Petrini (1992) in which they were exposed to 70% ethanol for 15 min, 40% NaOCl solution ($\approx$ 12% available chlorine when undiluted) for 15 min and 70% ethanol for 15 min. To check for sterility, the flow system was operated with sterile media for 3 days before inoculation. Sterility was confirmed by plating three 0.1 ml aliquot effluent samples onto King's B agar (King *et al*., 1954).

Microscopy and image analysis

The flow cells were positioned on a polycarbonate holder, which was mounted on the stage of an Olympus BH2 upright microscope. The biofilm growing on both the top and the bottom surfaces of the flow cells was imaged *in situ* using bright-field microscopy. The contrast was adjusted by changing the condenser height and the diaphragm aperture. A COHU 4612-5000 CCD camera and a Scion VG-5 PCI framestore board were used to capture images. Biofilm length dimensions were measured using Scion image, which is based on the public domain NIH-Image 1.59 program (internet address: rsb.info.nih.gov/nih-image). The height of the biofilm at the crest of the ripples was measured microscopically as described elsewhere (Bakke and Olsson, 1986). The ripple wavelength was measured as the peak-to-peak distance between two ripples in an axis parallel to the flow of the bulk liquid. Time-lapse imaging by frame-to-frame capture was used to determine temporal changes in biofilm structure and the velocity of ripple migration. A 1 mm graticule with 10 μm divisions (CS990; Graticules Ltd) was used for microscope calibration.

Inoculum and enumeration procedures

The inoculum contained *P. aeruginosa* (ERC1), *P. fluorescens*, *K. pneumoniae* and *S. maltophilia*. These Gram-negative species are commonly isolated from environmental and industrial biofilms and have been used as a reproducible model community in previous studies in our laboratory (Stoodley *et al*., 1999b). Stab inoculation of each species into 0.3% nutrient agar showed that *P. aeruginosa* (ERC1), *P. fluorescens* and *S. maltophilia* were motile, while *K. pneumoniae* was non-motile over a monitoring period of 24 h.

Frozen stock cultures (0.5 ml of 3×10^8 to 4×10^9 cfu ml^{-1}) of each of the four species were thawed and injected directly into the chemostat. The reactor was initially run as a recirculating batch culture for 24 h, before switching to continuous culture. Effluent samples were taken periodically to monitor the suspended population. Each of the four species could be identified (by colour and morphology) and enumerated by serial plating in triplicate on King's B agar with added bromthymol blue (BTB, 0.03 g l^{-1}) as a pH indicator (Stoodley *et al.*, 1999a). Because of overgrowth on the plates, individual species could only be detected in concentrations above 0.5% of the total population.

Nutrients

Biofilms were grown on a minimal salts medium consisting of 10 mg l^{-1} ammonium sulphate ($(NH_4)_2SO_4$), 70 mg l^{-1} potassium phosphate monobasic (KH_2PO_4), 30 mg l^{-1} potassium phosphate dibasic (K_2HPO_4) 10 mg l^{-1} and magnesium sulphate ($MgSO_4.7H_2O$), with glucose (40 mg l^{-1}) as the sole carbon source, and the following additional trace elements (concentration in mg l^{-1} in parentheses): $Na_2EDTA{\cdot}2H_2O$ (12); $FeSO_4{\cdot}7H_2O$ (2); $CaCl_2$ (1); Na_2SO_4 (1); $ZnSO_4{\cdot}7H_2O$ (4); $MnSO_4{\cdot}4H_2O$ (4); $CuSO_4{\cdot}5H_2O$ (1); $Na_2MoO_4{\cdot}2H_2O$ (1). The media was made in 10 l batches and sterilized by autoclaving at 121°C for 1 h; the final pH was 6.8. Dissolved oxygen (DO) was monitored periodically by a colorimetric method using R-7501 CHEMets ampoules (CHEMetrics). The DO concentration in the effluent did not fall below 1 mg l^{-1} during the course of the experiments.

Enumeration of viable biofilm bacteria

At the end of the experiments, the flow cells were removed from the reactor and rinsed five times with 1 ml of sterile buffer (quarter-strength Ringers' solution), sectioned with a diamond knife and immersed in 5 ml of sterile buffer with 0.1% (w/v) Tween 20. Samples were sonicated for 3×5 min and vortexed for 10 s between sonications. We estimated, by microscopic examination, that this method removed more than 98% of the biomass (Stoodley *et al.*, 1999b). Serial dilutions were plated onto King's B + BTB agar, incubated at 24°C and counted after 48 h.

Enumeration of viable cells in biofilm ripple bed

At the end of run 3, viable bacterial cells in two patches of biofilm ripples were enumerated by selective sampling with a micropipette (tip diameter 100 μm) attached to a peristaltic pump. The turbulent flow cell was removed from the reactor, and the outside was swabbed with 70% ethanol. The flow cell was then cut into lengths of ≈2 cm, and a section of glass was cut from the top surface with a diamond knife. The glass section was attached to the bottom of a Petri plate with double-sided tape, immersed in sterile Ringers' buffer and placed under a dissecting microscope. The micropipette was positioned (using a micromanipulator) over a large ripple bed. Suction was applied so that the ripples were drawn into the micropipette and transferred for serial plating. The sampled areas were circles of ≈300 μm diameter, 7.1×10^{-4} cm^2.

Acknowledgements

From Exeter University, we thank Luanne Hall-Stoodley for technical discussion and careful review of the manuscript, Tony Davey and Alan G. Hailey for their help with design and manufacture of the flow system, and Ian Dodds for assistance with experiments. This work was supported in part by the co-operative agreement ECD-8907039 with the Engineering Research Centers and Education Division of NSF.

References

Bakke, R., and Olsson, P.Q. (1986) Biofilm thickness measurements by light-microscopy. *J Microbiol Methods* **5:** 93–98.

deBeer, D., Stoodley, P., Roe, F., and Lewandowski, Z. (1994) Effects of biofilm structures on oxygen distribution and mass transfer. *Biotechnol Bioeng* **43:** 1131–1138.

Bryers, J., and Characklis, W.G. (1981) Early fouling biofilm formation in a turbulent flow system: overall kinetics. *Water Res* **15:** 483–491.

Buswell, C.M., Herlihy, Y.M., Lawrence, L.M., McGuiggan, J.T.M., Marsh, P.D., Keevil, C.W., *et al.* (1998) Extended survival and persistence of Campylobacter spp. in water and aquatic biofilms and their detection by immunofluorescent-antibody and -rRNA staining. *Appl Environ Microbiol* **64:** 733–741.

Caldwell, D.E., Korber, J.R., and Lawrence, D.R. (1993) Analysis of biofilm formation using 2D vs. 3D digital imaging. *J Appl Bacteriol* **74:** S52–S66.

Carpentier, B., and Cerf, O. (1993) Biofilms and their consequences, with particular reference to hygiene in the food industry. *J Appl Bacteriol* **75:** 499–511.

Characklis, W.G. (1981) Fouling biofilm development: a process analysis. *Biotechnol Bioeng* **23:** 1923–1960.

Characklis, W.G. (1990) Process analysis in biofilms. In *Biofilms*. Characklis, W.G., and Marshall, K.C. (eds). New York: Wiley, pp. 17–54.

Costerton, J.W., Lewandowski, Z., Caldwell, D.E., Korber, D.R., and Lappin-Scott, H.M. (1995) Microbial biofilms. *Annu Rev Microbiol* **49:** 711–745.

Davies, D.G., Marsek, M.R., Pearson, J.P., Iglewski, B.H., Costerton, J.W., and Greenberg, E.P. (1998) The involvement of cell-to-cell signals in the development of a bacterial biofilm. *Science* **210:** 295–298.

Fisher, P.J., and Petrini, O. (1992) Fungal saprobes and pathogens as endophytes of rice (*Oryza sativa* L.). *New Phytol* **120:** 137–143.

Foley, I., and Gilbert, P. (1996) Antibiotic resistance of biofilms. *Biofouling* **104:** 331–346.

Gjaltema, A., Arts, P.A.M., van Loosdrecht, M.C.M., Kuenen, J.G., and Heijnen, J.J. (1994) Heterogeneity of biofilms in rotating annular reactors: occurrence, structure, and consequences. *Biotechnol Bioeng* **44:** 194–204.

Hoiby, N., Fomsgaard, A., Jensen, E.T., Johansen, H.K., Kronborg, G., Pedersen, S.S., *et al.* (1995) The immune response to bacterial biofilms. In *Microbial Biofilms.* Plant and Microbial Biotechnology Research Series 5. Lappin-Scott, H.M., and Costerton, J.W. (eds). Cambridge: Cambridge University Press, pp. 233–250.

King, O.E., Ward, M.K., and Raney, D.E. (1954) Two simple media for the demonstration of pyocyanin and fluorescein. *J Lab Clin Med* **44:** 301–307.

Lappin-Scott, H.M., and Costerton, J.W. (1989) Bacterial biofilms and surface fouling. *Biofouling* **1:** 323–342.

McCoy, W.F., Bryers, J.D., Robbins, J., and Costerton, J.W. (1981) Observations of fouling biofilm formation. *Can J Microbiol* **27:** 910–917.

Massol-Deya, J., Whallon, R.F., Hickey, J.M., and Tiedje (1994) Channel structures in aerobic biofilms of fixed-film reactors treating contaminated groundwater. *Appl Environ Microbiol* **61:** 769–777.

Møller, S., Sternberg, C., Andersen, J.B., Christensen, B.B., Ramos, J.L., Givskov, M., *et al*. (1998) *In situ* gene expression in mixed-culture biofilms: evidence of metabolic interactions between community members. *Appl Environ Microbiol* **64:** 721–732.

Palmer, R.J., and White, D.C. (1997) Developmental biology of biofilms: implications for treatment and control. *Trends Microbiol* **11:** 435–440.

Picioreanu, C., van Loosdrecht, M.C.M., and Heijnen, J.J. (1998) Mathematical modeling of biofilm structure with a hybrid differential-discrete cellular automaton approach. *Biotechnol Bioeng* **58:** 101–116.

Picologlou, B.F., Zelver, N., and Characklis, W.G. (1980) Biofilm growth and hydraulic performance. *J Hydraul Div Am Soc Civ Eng* **106 (HY5):** 733–746.

Reichert, P., and Wanner, O. (1997) Movement of solids in biofilms: significance of liquid phase transport. *Water Sci Technol* **36:** 321–328.

Stoodley, P., Boyle, J.D., Dodds, I., and Lappin-Scott, H.M. (1997) Consensus model of biofilm structure. In *Biofilms: Community Interactions and Control.* Wimpenny, J.W.T., Handley, P.S., Gilbert, P., Lappin-Scott, H.M., and Jones, M. (eds). Cardiff: BioLine, pp. 1–9.

Stoodley, P., Lewandowski, L., Boyle, J.D., and Lappin-Scott, H.M. (1998) Oscillation characteristics of biofilm streamers in turbulent flowing water as related to drag and pressure drop. *Biotechnol Bioeng* **57:** 536–544.

Stoodley, P., Lewandowski, Z., Boyle, J.D., and Lappin-Scott, H.M. (1999a) Structural deformation of bacterial biofilms caused by short term fluctuations in flow velocity: an *in-situ* demonstration of biofilm viscoelasticity. *Biotechnol Bioeng* **65:** 83–92.

Stoodley, P., Dodds, I., Boyle, J.D., and Lappin-Scott, H.M. (1999b). Influence of hydrodynamics and nutrients on biofilm structure. *J Appl Microbiol* **85** 19S–28S.

Stoodley, P., Dodds, I., Boyle, J.D., and Lappin-Scott, H.M. (1999c) Influence of flow on the structure of bacterial biofilms. In *Microbial Biosystems: New Frontiers.* Bell, C.R., Brylinsky, M., and Johnson-Green, P. (eds). Proceedings of the 8th International Symposium on Microbial Ecology. Atlantic Canada Society for Microbial Ecology.

Vogel, S. (1994) *Life in Moving Fluids*, 2nd edn. Princeton, NJ: Princeton University Press.